ESTIMATION OF THE CHARACTERIZATION ACCURACY OF A THIN NONABSORBING FILM BY MULTIPLE-ANGLE-OF-INCIDENCE ELLIPSOMETRY

I.S. PETRIK, A.V. TURCHIN[1], E.K. FROLOVA[1]

UDC 535.32

Institute of Surface Chemistry, Nat. Acad. Sci. of Ukraine
(17, General Naumov Str., Kyiv 03164, Ukraine),
[1]**Institute of Physics, Nat. Acad. Sci. of Ukraine**
(46, Nauka Ave., Kyiv 03028, Ukraine; e-mail: turchin@iop.kiev.ua)

While determining the parameters of thin nonabsorbing films experimentally, making use of the method of multiple-angle-of-incidence ellipsometry (MAIE), a drastic decrease of the characterization accuracy has been found for some specimens. In order to study this effect, we introduced the error function of a new type that has a clear physical meaning of the "averaged neglected photocurrent" and, on its basis, built a procedure for the numerical solution of the inverse problem of ellipsometry. The treatment of experimental data making use of this procedure enabled the boundaries of the region of admissible parameters (RAP) to be determined for a number of porous TiO_2 film specimens. Furthermore, the numerical calculations showed that the accuracy of the ellipsometric film characterization depends on the film parameters in an oscillatory manner. The results obtained have demonstrated that the stage of numerical calculations of the RAP boundaries has to be included into the procedure of solving the inverse problem of ellipsometry.

1. Introduction

The progress in applying thin films in various physical, chemical, and technical tasks is governed, to a great extent, by the quality and the veproducibility of the films with such designated parameters as the refractive index, absorption coefficient, thickness, and film homogeneity. In order to check the film parameters in a nondestructive manner and to correct the conditions of a technological process in the course of the thin film fabrication, it is convenient to use the method of ellipsometry which is based on the analysis of the variation of the monochromatic light polarization, when light interacts with the surface of a specimen. Zero-ellipsometry, which is not a direct experimental method for measuring the refractive index n and the thickness d of the film, is most often used. Therefore, in order to find the required physical properties of a film, one has to solve the inverse problem of ellipsometry. However, it is customary to assume [1–5] that, in the case of a homogeneous, isotropic, non-absorbing film with sharp film–substrate and film—air interfaces, the use of MAIE allows both n and d to be determined unambiguously, with probable complications, if they do arise while solving the inverse problem, being relevant only for very thin films.

Having developed the MAIE method and created a numerical code that can solve the inverse ellipsometric problem, we carried out a number of measurements of nano-sized non-absorbing substances, which had been deposited as single- and multilayer films onto substrates. The reliability of the n and d values obtained was verified by comparing them with the data of spectral measurements carried out for the same specimens [6]. As a rule, the MAIE results correlated well with the spectral ones. However, at some thicknesses, a substantial difference (up to 10%) between the values of the refractive index n measured by those two methods was revealed. An assumption arose that, provided a definite relationship between n and d, the accuracy of the solution of the inverse problem for MAIE becomes considerably worse.

In this connection, in this work, we have studied the accuracy of the ellipsometric characterization of thin non-absorbing films by the MAIE method. We also searched for possible experimental situations, in

which the accuracy concerned decreases substantially. In so doing, we have developed a numerical technique for estimating the errors of the determination of the refractive index and the film thickness from experimental data.

2. Experimental Part

2.1. Fabrication of specimens

Sol-gel solutions (precursors) for porous TiO_2 films were prepared making use of α-terpineol, in order to substantially enhance the viscosity of the solution, and PEG600 (Loba feinchemie) as a porophore. Acetic acid (Ukrreakhim) was added to the solution as an acid catalyst. For a film precursor, two solutions, A and B, were prepared. Solution A was the mixture of 0.34 M of Ti tetraisopropoxide (97%, Aldrich), 3.26 M of isopropyl alcohol (Ukrreakhim), 2.12 M of α-terpineol, and a porophore. Solution B consisted of the following components: isopropyl alcohol, distilled water, and acetic acid. Provided continuous stirring, solution B was added dropwise to solution A. The concentration of TiO_2 in the solution was 4 wt.%.

The films were drawn from the solution obtained at a rate of about 9 cm/min onto glass substrates with the refractive index $n_2 = 1.516$; the substrates, before the film deposition, were carefully washed clean in hydrochloric acid and distilled water and dried in a drying cabinet at $t = 150°$C. After the deposition of the precursor onto substrates, the film was warmed thoroughly for an hour at a temperature of 500°C.

2.2. Measurement procedure

Measurements were carried on making use of a LEF-3M-1 zero-ellipsometer. A laser beam with the wavelength $\lambda = 0.6328$ μm and circular polarization passes first through a polarizer (P) and a compensator (C). Having been reflected specularly from the specimen at an angle ϕ, it passes through an analyzer (A) to be registered by a detector. The ellipsometric azimuths P, C, and A describe the angles of counterclockwise rotation of the corresponding elements around the current axis of the laser beam, if one looks towards the beam; they are reckoned from the plane of incidence.

The reflection of light by a specimen covered with an isotropic film is completely described by a diagonal matrix $R(\phi, \Pi)$, the elements of which are, generally speaking, the complex coefficients of reflection of the p- and s-polarized light, $R_p(\phi, \Pi)$ and $R_s(\phi, \Pi)$,respectively. Here, $\Pi = (\varepsilon_0, \varepsilon_1, \varepsilon_2, d)$ stands for a set of physical quantities which completely describe the reflecting structure; namely, ε_0, ε_1, and ε_2 are the dielectric permittivities of air, the film, and the substrate, respectively; and d is the film thickness. In such a geometry of measurements, the amplitude of the electric field of a light wave at the detector looks like [1]

$$E(P, A, g, \phi, \Pi) = E_{\text{in}} Q(P, A, g, \phi, \Pi). \tag{1}$$

Hereafter, we consider the most widespread experimental case, where the compensator is fixed in one of two positions: $C = 45°g$, where $g = \pm 1$. The quantity E_{in} designates the amplitude of the wave after its having passed the polarizer, while the dimensionless multiplier $Q(P, A, g, \phi, \Pi)$ is determined by the variation of polarization, when light passes the whole optical path, and can be written down in terms of the matrix product as

$$Q(P, A, g, \phi, \Pi) = (\cos A \sin A) \times$$

$$\times \begin{pmatrix} R_p(\phi, \Pi) & 0 \\ 0 & R_s(\phi, \Pi) \end{pmatrix} \begin{pmatrix} \exp(ig(P - \pi/4)) \\ \exp(-ig(P - \pi/4)) \end{pmatrix}. \tag{2}$$

The photocurrent through the detector is determined by the formula

$$I(P, A, g, \phi, \Pi) = kE_{\text{in}}^2 \cdot Q(P, A, g, \phi, \Pi) Q^*(P, A, g, \phi, \Pi) =$$

$$= I_0 |(P, A, g, \phi, \Pi)|^2, \tag{3}$$

where the asterisk denotes complex conjugation, while the physical meaning of the quantities k and I_0 is obvious. In this case, the condition that no light falls down onto the surface,

$$Q(P, A, g, \phi, \Pi) = 0, \tag{4}$$

is often expressed in terms of the complex-valued ratio $\rho(\phi, \Pi) = R_p(\phi, \Pi)/R_s(\phi, \Pi)$ between the reflection coefficients of p- and s-polarized light, which looks like

$$\rho(\phi, \Pi) = -\operatorname{tg} A \exp(-ig2(P - \pi/4)). \tag{5}$$

Experimental results are usually presented in the form of the dependences $\Psi(\phi)$ and $\Delta(\phi)$, where the ellipsometric angles Ψ and Δ are defined by the relationship

$$\rho = \operatorname{tg} \Psi \exp(i\Delta). \tag{6}$$

We also note that the procedure of comparison of experimental data with the results of model calculations, which was applied in this work, deals only with the dependences of the azimuths $P(\phi)$ and $A(\phi)$ that have been directly measured in experiment, while the angles Ψ and Δ are used only to illustrate the results obtained.

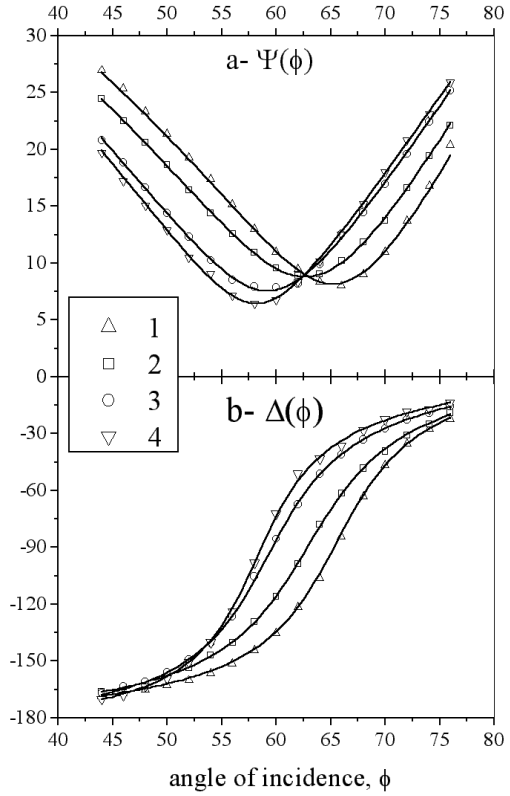

Fig. 1. Dependences of the ellipsometric angles Ψ (a) and Δ (b) on the angle of incidence ϕ for four sections (numbered by 1 to 4) of the same specimen. The symbols correspond to experimental data, and the solid curves to model calculations making use of the parameters $h_m = d/\lambda$ and n_m found by solving the inverse problem (see Table)

2.3. Results of measurements

In order to illustrate the experimental results, we selected four sections of the same specimen. In this case, we might expect for the invariance of the refractive index and a certain variation of the selected sections by thickness, although the weak influence of the film thickness on its porosity and, as a consequence, on its refractive index still remains. The results of measurements are exposed in Fig. 1 in the form of the dependences $\Psi(\phi)$ and $\Delta(\phi)$. In order to minimize errors, the measurements were carried on at various angles of incidence ϕ_i (in the interval from 44 to 78° with a step of 2°), and every experimental point was obtained by averaging over nonequivalent positions with the absence of light at the detector. With this purpose in view, two sets of the azimuths (P_j, A_j) were measured at each fixed azimuth of the compensator ($C = \pm 45°$), at which there was no light at the detector, and the corresponding values of $\rho_j(\phi)$ were found by formula (5). The ellipsometric angles $\Psi(\phi)$ and $\Delta(\phi)$ were calculated, basing on the averaged value

$$\rho(\phi) = \frac{1}{4}\sum_{j=1}^{4}\rho_j(\phi). \tag{7}$$

3. Model and the Calculation Procedures

3.1. Solution of the inverse ellipsometric problem

While calculating the dimensionless parameters of the film – its reduced thickness $h = d/\lambda$ and dielectric permittivity ε_1 – from experimental MAIE data, we supposed the substrate to be thick enough for the light, which was reflected from its back side, not to fall on the detector, and the dielectric permittivities ε_0 and ε_2 to be known. Though the system under consideration — air—film—glass — is rather simple, there is no analytical solution for this inverse problem. Therefore, the numerical calculations consisting of three routines were carried out.

The first routine (the basic routine) solves the direct problem of determining the reflection coefficient $R_p(\varepsilon_0, \varepsilon_1, \varepsilon_2, h, \phi)$ and $R_s(\varepsilon_0, \varepsilon_1, \varepsilon_2, h, \phi)$, knowing the preassigned values for the (h, ε_1) pair of film parameters at every angle of light incidence ϕ_i.

The second routine (the routine of comparison), making use of the error function (see below), calculates first a discrepancy between the set of experimental MAIE data and the results of simulation for the given set of film parameters (h, ε_1) for every angle of light incidence. Afterwards, it evaluates the error, averaged over all the angles of incidence, as a single number S.

At last, the third routine (the routine of minimization) operates with the dependence of the average error S on the model parameters (h, ε_1) and, using a procedure of minimization, which is based on the Levenberg—Marquadt iteration method, obtains the solution of the inverse problem in the form of a pair of numbers (h_m, ε_{1m}), at which the error acquires the minimal value $S_{\min}$.

We emphasize that all dielectric permittivities in this work are real-valued quantities. Therefore, in

what follows, we characterize the film by the pair of parameters (h, n), where n is the refractive index of the film.

3.2. Solution of the direct problem

The problem of determination of the reflection coefficients R_p and R_s of a monochromatic wave from a layered structure, which is formed by plane-parallel homogeneous layers with isotropic properties and sharp interfaces, has been considered in a lot of works [1, 7, 8]. We applied an approach, which, on the one hand, is the most general and, on the other hand, allows structures possessing an arbitrary number of layers to be included into consideration in a natural way. The approach is based on the circumstance [9] that a plane monochromatic electromagnetic wave, while falling onto a layered structure, excites two plane inhomogeneous waves (refracted and reflected) for both polarizations (s- and p-) in each of its layers; the spatial part of each excited wave is described by a, generally speaking, complex wave vector

$$\mathbf{k} = Re\mathbf{k} + iIm\mathbf{k} = \mathbf{k}_R + i\mathbf{k}_I. \tag{8}$$

In this case, the system of Maxwell equations for a separate layer can be solved only if

$$\mathbf{k}^2 = \mathbf{k}\cdot\mathbf{k} = \mathbf{k}_R^2 - \mathbf{k}_I^2 + i2\mathbf{k}_R\cdot\mathbf{k}_I = \varepsilon\mu\frac{\omega^2}{c^2} = \varepsilon\frac{\omega^2}{c^2}. \tag{9}$$

The last equality means that the magnetic permeability of the medium μ, as is usually done for high-frequency fields, should be put equal to unity [9].

In the framework of our approach, the key variables of the problem are the complex amplitudes of inhomogeneous plane waves. Two amplitudes, which describe the waves of the same polarization in the same layer, form a column vector. In this case, the column vectors of different polarizations are not connected with one another, while the column vectors of identical polarizations in the neighbor layers are transformed into one another by means of a 2×2-matrix, the elements of which are defined by standard boundary conditions for the fields E and B.

3.3. Error function

As usual, the measurements are aimed at finding the most probable value of a physical quantity F_m and at estimating the limits of the interval which includes the value measured. An inherent feature of ellipsometry is that a separate measurement necessarily demands the simultaneous measurements of two quantities, P and A, and the purpose is both finding the most probable value of the physical constants of the film (h_m, n_m) and estimating the boundaries of the RAP in the $h-n$ plane; every point of the RAP ensures that the error of measurements is within the preset limits. The value of the difference $F_i - F_m$ is practically always taken for the error of a separate i-th measurement, and the most probable value F_m on multiple measurements is selected to minimize the sum of $(F_i - F_m)^2$ terms over all measurements. In the case of ellipsometry, there is an ambiguity in the choice of a common error function. This function should provide a numerical criterion of how well the experimental data (e.g., the set of triplets $M^i_{\rm exp} = (\phi_i, P_i, A_i)$) correspond to the model concepts (in our case, we have the set of model parameters $M^i_{\rm mod} = (\phi_i, h, n)$); in such a way, it should ensure the verification of the solutions of both the problems stated above.

Let us specify the basic requirements which should be satisfied by the error function. Its arguments have to be $M^i_{\rm exp}$ and $M^i_{\rm mod}$. Its result must be a real number. Provided that the arguments perfectly coincide, the function must equal zero; while at their small mismatch, the result of the function has to be expressed in terms of a positive definite quadratic form of the mismatch amplitude. In addition, it is desirable that the function should be closely connected to a quantity that is directly measured in experiment.

The error functions, which are described in the literature [1–3, 10, 11], belong to one of two types, depending on the physical quantities which are used for the comparison of experimental data with simulation ones. If the complex-valued ratio between the reflection coefficients for light with p- and s-polarizations is used, the error function looks like

$$F_\rho(\{M^i_{\rm exp}\}, \{M^i_{\rm mod}\}) =$$

$$= \Sigma_i |\rho_{\rm exp}(M^i_{\rm exp}) - \rho_{\rm mod}(M^i_{\rm mod})|^2. \tag{10}$$

The ellipsometric angles Ψ and Δ are used more often for comparison. In this case, the error function is written down in the form

$$F_{\Psi\Delta}(\{M^i_{\rm exp}\}, \{M^i_{\rm mod}\}) =$$

$$= \Sigma_i \big\{ (\Psi_{\rm exp}(M^i_{\rm exp}) - \Psi_{\rm mod}(M^i_{\rm mod}))^2/\sigma^2_\Psi +$$

$$+(\Delta_{\text{експ}}(M^i_{\text{exp}}) - \Delta_{\text{mod}}(M^i_{\text{mod}}))^2/\sigma^2_\Delta\}, \quad (11)$$

with the definitions of the coefficients σ_Ψ and σ_Δ by various authors differing from one another. This work does not aim at comparing various types of the error function. Therefore, we confine ourselves to the general statement that the question concerning the optimal form of the error function has not been answered yet, and the corresponding answer could be obtained only after carrying out an additional and very cumbersome experiment.

Our procedure is based on the error function of a new type, which, to our knowledge, has not been mentioned earlier in the literature. Since the ultimate measured quantity is the photocurrent through a detector, any discrepancy between the measurement and simulation data, whatever experimental circumstances or model imperfections may cause it, can be reduced to the effective photocurrent. From this reason, it is natural to describe the agreement between experimental data and model parameters in the form of a photocurrent through the detector in a gedankenexperiment, where the angle of light incidence and the positions of the polarizer and the analyzer are described by the experimental set M^i_{exp}, while the matrix of light reflection, provided the given angle of incidence, is described by the model set M^i_{mod}. One may assert that the function that has been introduced in such a manner has the sense of an "averaged neglected photocurrent", and its explicit form has to depend on both the type of the ellipsometric experiment and the details of the layered structure. For the air—film—substrate structure considered above, the suggested error function looks like

$$F_I(\{M^i_{\text{exp}}\}, \{M^i_{\text{mod}}\}) =$$

$$= N^{-1} \sum_i |Q(P_i, A_i, g, \phi_i, h, n, \varepsilon_0, \varepsilon_2)|^2 =$$

$$= N^{-1} \sum_i \Bigg| (\cos(A_i)\sin(A_i)) \times$$

$$\times \begin{pmatrix} R_p(\phi_i, h, n, \varepsilon_0, \varepsilon_2) & 0 \\ 0 & R_s(\phi_i, h, n, \varepsilon_0, \varepsilon_2) \end{pmatrix} \times$$

$$\times \begin{pmatrix} \exp(ig(P_i - \pi/4)) \\ \exp(-ig(P_i - \pi/4)) \end{pmatrix} \Bigg|^2 = S(h, n). \quad (12)$$

We have defined it, making use of expressions (2) and (3), with an accuracy to a constant dimensional multiplier. One can see that the error function depends explicitly on both the parameters that define a configuration of the ellipsometric experiment (P_i, A_i, and ϕ_i) and the parameters of the model (h, n, ε_0, and ε_2). The last equality in the chain of equations (12) is the definition of the average error depending on the film parameters. It is this dependence that is the most important while searching for the optimal solution (h_m, n_m) of the inverse problem.

3.4. Evaluation of the RAP boundaries

Making use of the surface $S(h, n)$, which was introduced in Eq. (12), the second posed problem — to evaluate the region of admissible parameters – can be solved. For this purpose, let us pay attention to the physical meaning that can be assigned to the quantity $S^{\min}$. Writing down the error function in form (12), we identify each of its terms with a squared module of the electric field at the detector (see Eq. (1)) in the gedankenexperiment. In so doing, we ascribe the meaning of the root-mean-square deviation of the electric field from zero in the gedankenexperiment to the whole error function. But in this case, it is the minimum value on the error surface that determines this deviation σ^2_E:

$$S^{\min} = S(h_m, n_m) = \sigma^2_E. \quad (13)$$

On the other hand, if the experimental sample contains $N + 1$ measurements, the root-mean-square error of the sample average amounts to σ^2_E/N. Therefore, hereafter, we determine the RAP by the sample average criterion, assuming that this region covers the portion of the plane, for which the error function does not exceed such a value S^σ that

$$S^{\min} < S(h, n) < S^\sigma = \sigma^2_E(1 + 1/N) = S^{\min}(1 + 1/N). \quad (14)$$

4. Comparison of Experimental Data with the Results of Simulation Calculations

4.1 4.1. Solution of the inverse problem

The procedure for solving the inverse problem of ellipsometry which was described above was applied to treat the experimental data exposed in Fig. 1. The optimal parameters of the model (h_m, n_m), at which the fitting of the experimental curves is the best, are quoted in the table. The corresponding fitted curves $\Psi(\phi)$ and $\Delta(\phi)$ are also plotted in the same figure by solid curves.

4.2. Regions of admissible parameters

For every section of the specimen, we numerically calculated a region around (h_m, n_m), all points of which satisfied condition (14). The results of calculations are summarized in Fig. 2 in the form of the boundaries of the corresponding RAPs; they provide the exhaustive information concerning the ranges of parameters which describe well each pair of the experimental curves in Fig. 1. It is evident that each region is approximated well by a very prolate ellipse, for the satisfactory description of which only the values of the major (D_h) and minor (d_h) semi-axes, as well as the slope angle β of the major semi-axis with respect to the axis n, should be specified. In order to calculate them, let us expand the error function in a series in the vicinity of its minimum up to the quadratic terms, making use of the matrix $S_{,hn}$ composed of the second derivatives:

$$S(h,n) = S^{\min} + \frac{1}{2}(h-h_m n-n_m)\times$$

$$\times \begin{pmatrix} S_{,hh} & S_{,nh} \\ S_{,hn} & S_{,nn} \end{pmatrix} \begin{pmatrix} h-h_m \\ n-n_m \end{pmatrix}. \qquad (15)$$

By equating the right-hand side of Eq. (15) to the value of S^{σ} from relationship (14), we obtain the required expressions as

$$D_h = \frac{2\sigma_E}{\sqrt{N}}\left[(S_{,hh}+S_{,nn})+\right.$$

$$\left.+\sqrt{(S_{,hh}-S_{,nn})^2+(2S_{,hn})^2}\right]^{-1/2}, \qquad (16a)$$

$$d_h = \frac{2\sigma_E}{\sqrt{N}}\left[(S_{,hh}+S_{,nn})+\right.$$

$$\left.+\sqrt{(S_{,hh}-S_{,nn})^2+(2S_{,hn})^2}\right]^{-1/2}, \qquad (16b)$$

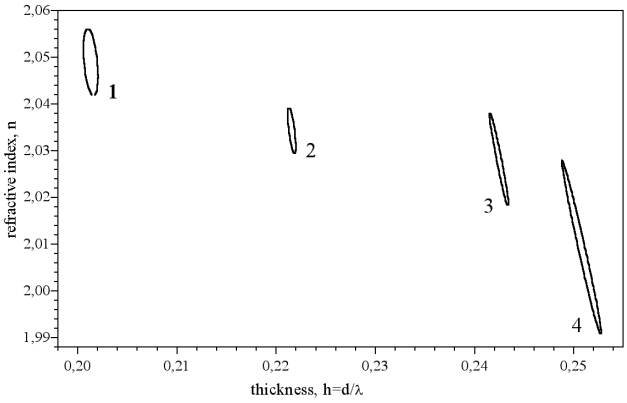

Fig. 2. The regions of admissible parameters calculated in accordance with the average sample criterion (see Eqs. (13) and (14)) for each of the four sections (*1–4*)

$$\beta = 1/2\,\mathrm{arctg}\left(\frac{S_{,hh}-S_{,nn}}{2S_{,hn}}\right) - \pi/4. \qquad (16c)$$

The values of the key parameters, which describe each of the regions shown in Fig. 2, are quoted in the table. They were determined by expressions (16a)—(16c). The second derivatives which compose the matrix $S_{,hn}$ were found by constructing a two-dimensional polynomial interpolation of the function $S(h,n)$ near the point (h_m, n_m). The table also includes the amplitudes of the errors σ_E and $\sigma_N = \sigma_E/\sqrt{N}$, as well as the values of the ratios D_h/σ_N and d_h/σ_N.

We emphasize the following results. The ratio d_h/σ_N changes little, if at all; therefore, it is the transverse size of the RAP that is determined by the experimental parameter σ_N. On the other hand, the ratio D_h/σ_N changes strongly over the various sections of the specimen, which means a strong dependence of the RAP diameter $(2D_h)$ not only on the experimental error σ_N, but also on the physical parameters of the section.

Serial No. of the section	1	2	3	4
Refractive index of the film, n_m	2.049	2.034	2.028	2.009
Reduced thickness $h_m = d/\lambda$	0.2013	0.2215	0.2425	0.2508
Average neglected photocurrent, $S^{\min} = \sigma_E^2$	$(0.00492)^2$	$(0.00232)^2$	$(0.00212)^2$	$(0.00305)^2$
$\sigma_N = \sigma_E/\sqrt{N}$	0.00123	0.00058	0.00053	0.00076
Major semi-axis of the RAP, D_h	0.00723	0.00511	0.00982	0.01889
Minor semi-axis of the RAP, d_h	0.00067	0.00030	0.00024	0.00035
Slope angle of the ellipse, β	−0.0406	−0.0572	−0.0921	−0.1046
D_h/σ_N	5.88	8.81	18.49	24.78
d_h/σ_N	0.54	0.51	0.45	0.46

5. Discussion of Experimental Results

Analyzing the results presented in Figs. 1 and 2, as well as in the table, one can draw some conclusions concerning the film parameters and the technology of film fabrication. In particular, the refractive index can be considered to vary little, if at all, while the thickness of the film produced using this technology changes substantially, at least from 0.2013 to 0.2508 Å.

The most interesting, however, seem the data for the ratio D_h/σ_N. One of these parameters, σ_N, according to Eq. (13), is determined by a discrepancy between experimental and simulation results. If the model describes the observations correctly, it is this parameter that characterizes the experimental errors. At the same time, the ultimate accuracy of MAIE, if the latter is considered as the method to characterize thin films, is determined by the diameter $2D_h$ of that region of parameters, every point of which brings experimental and simulation results closer together, within the limits that are determined by the error function value. The data quoted in the table evidence for a strong dependence of the ratio D_h/σ_N on the physical parameters of the measured section of the film. Therefore, the assumption stated in Introduction that the accuracy of the solution of the inverse problem may decrease (this is attested by the growth of D_h), provided a relatively constant level of experimental errors (the parameter σ_N), becomes confirmed. The remaining part of the article is devoted to studying this effect.

According to Eq. (16a), we introduce the factor of proportionality G between the parameters σ_N and D_h:

$$D_h = G\sigma_N. \tag{17}$$

However, according to the procedure of calculations, the factor G is governed by the shape of the surface $S(h,n)$ which, in its turn, is calculated from experimental data. Hence, there appears the assumption that both the factor G and the shape of the RAP may depend on the magnitude of the error σ_N. In this connection, consider the terms of the function $S(h,n)$ in expression (12) separately. Let the model adequately describe the experiment, and the ellipsometric azimuths P_{im} and A_{im} correspond to the optimal parameters h_m and n_m at the angle of incidence ϕ_i. In this case, one may expand the multiplier $Q(P_i, A_i, g, \phi_i, h, n, \varepsilon_0, \varepsilon_2)$, which determines the electric field in the gedankenexperiment, in a series and keep only linear terms:

$$\mathrm{Q(P_i, A_i, g, \phi_i, h, n, \varepsilon_0, \varepsilon_2)} =$$

$$= (P_i - P_{im})\partial_P Q + (A_i - A_{im})\partial_A Q +$$

$$+(h - h_m)\partial_h Q + (n - n_m)\partial_n Q \partial_n Q, \tag{18}$$

where the notation $\partial_P Q_i$ stands for the partial derivative of the function Q with respect to the parameter P calculated at a point that describes the i-th gedankenexperiment. For the average error $S(h,n)$, we obtain

$$S(h,n) =$$

$$= N^{-1}\sum_i |(P_i - P_{im})\partial_P Q_i + (A_i - A_{im})\partial_A Q_i|^2 +$$

$$+(h - h_m)N^{-1}\sum_i \big[\big((P_i - P_{im})\partial_P Q_i + (A_i - A_{im})\times$$

$$\times\partial_A Q_i\big)\partial_h Q_i^* + \text{c.c.}\big] + (n - n_m)N^{-1}\times$$

$$\times\sum_i \big[((P_i - P_{im})\partial_P Q_i + (A_i - A_{im})\partial_A Q_i)\,\partial_n Q_i^* +$$

$$+\text{c.c.}\big] + (h - h_m)^2 N^{-1}\sum_i \partial_h Q_i \cdot \partial_h Q_i^* +$$

$$+(n - n_m)^2 N^{-1}\sum_i \partial_n Q_i \cdot \partial_n Q_i^* + (h - h_m)\times$$

$$\times(n - n_m)N^{-1}\sum_i [\partial_h Q_i \cdot \partial_n Q_i^* + \text{c.c.}]\,. \tag{19}$$

In this expression, the second and third terms correspond to a shift of the minimum position with respect to the point (h_m, n_m). If there are no regular experimental errors, these terms can be neglected. The first term determines a discrepancy between the experiment and the model, giving the value of the function $S(h,n)$ in its minimum (see Eq. (15)). Three other terms determine the members of the matrix $S_{,hn}$ and do not depend on experimental data; we designate their sum as $S_0(h,n)$. Thus, provided that the deviations are small, one may consider that

$$S(h,n) = S_0(h,n) + S^{\min} = S_0(h,n) + \sigma_E^2. \tag{20}$$

Therefore, the proportionality factor G, as well as the RAP shape, does not depend on the error value σ_N in the framework of the small error approximation, being determined only by the parameters of the model and the set of the angles of incidence.

6. Study of the RAP Shape and Diameter

Consider now the results of numerical calculation of the RAP shape and diameter, which are to be expected in experiment if the film is characterized by the dimensionless parameters h_m and n_m. Let us analyze the dependences of the shape and the diameter on those parameters. For the convenience of comparison, we take advantage of the approximation of small deviations (20) and consider that all necessary information concerning the spread of experimental data is contained in the single parameter σ_N. The set of the angles of light incidence $\{\phi_i\}$, which is used in calculations, is identical to the experimental conditions. Our task consists in finding such a region, in which, according to Eq. (14),

$$S_0(h,n) \le \sigma_N^2. \tag{21}$$

This problem can be solved by taking the corresponding derivatives of expression (19). However, it is easier to take advantage of the circumstance that the function $S_0(h,n)$ can be calculated immediately from expression (12) under the assumption that the experimental values of the ellipsometric azimuths are precisely equal to the values of P_{im} and A_{im}. The first series of calculations, which are presented below, was carried out just in such a manner.

This series of calculations was aimed at researching the dependence of the RAP shape on the film thickness. For this purpose, we set the refractive index of the film $n_m = 2.1$, and the film thickness h_m was varied from 0.01 to 7 with an increment of 0.01. The value of σ_N was taken 0.001. For every pair (h_m, n_m), the boundary of the region that surrounds the corresponding point (h_m, n_m) on the $h-n$ plane and satisfies inequality (21) was calculated. The first 100 regions (at $h_m \le 1$) are shown in Fig. 3 (panel *a*). The transverse sizes of these regions cannot be distinguished on this scale; therefore, a portion of Fig. 3,*a*, scaled up in the h-axis direction, is presented in panel *b*.

It is evident that every region is a strongly prolate ellipse. The minor semi-axes of these ellipses depend on the film thickness weakly, if at all. In the case of the given value of σ_N, the minor semi-axes are approximately equal to 0.0005 and become somewhat shorter as the thickness increases. On the contrary, the dependence of the major semi-axis on the film thickness strongly oscillates, being more than an order of magnitude larger if the reduced film thickness amounts to an integral multiple of 0.263. For example, the length of the major semi-axis changes from 0.003 at $h_m = 0.13$ to more than 0.1 at $h_m = 0.26$. Moreover, the growth of

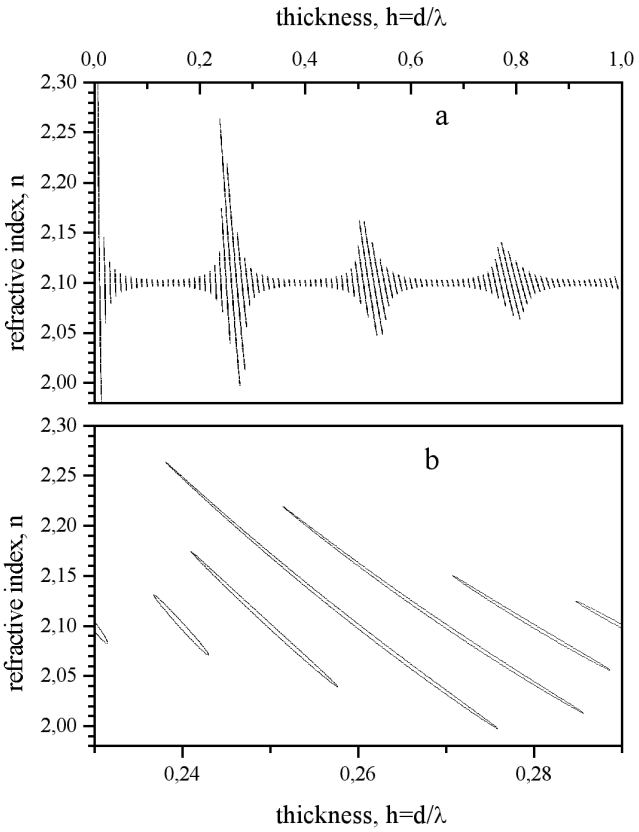

Fig. 3. (*a*) Results of calculations of the RAP shape for some pairs of the parameters (h_m, n_m) (see in the text). (*b*) The portion of panel *a* scaled up along the h-axis to demonstrate the transverse dimensions of the regions

the region is accompanied by the appreciable bending of its shape. As the film thickness increases, oscillations become smoother; and, approximately above $h_m = 5$, the length of the major semi-axis decreases gradually and monotonically. The slope of the major semi-axis of the ellipse is determined mainly by the constancy of phase retardation across the film.

The second series of calculations was aimed at researching the dependence of the RAP diameter on both film parameters. Now, in order to calculate the half diameter, we used expression (16a). The second derivatives, which compose the matrix $S_{,hn}$, were determined by carrying out a two-dimensional polynomial interpolation of the function $S_0(h,n)$ in the vicinity of the (h_m, n_m) point. Certainly, this method is an approximation in comparison with the straightforward numerical calculation of the region shape that was fulfilled in the first series of calculations,

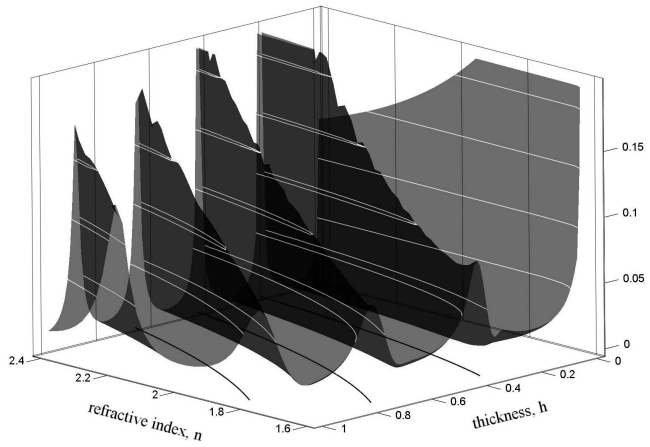

Fig. 4. Dependence of the major semi-axis D_h on the film parameters h_m and n_m (the translucent surface). Light curves on the surface are the contours of constant D_h. Three curves in the $h-n$ plane satisfy the empirical condition (22) and interpolate the positions of surface crests

and this deforms the final result a little. However, the results deviate from each other only in the vicinity of maximal diameters, and the discrepancies, as is seen from Fig. 3, are not large. Here again, $\sigma_N = 0.001$.

The results of calculations of the half diameter are exposed in Fig. 4. The refractive index of the film n_m was changed in the range from 1.6 to 2.4, and the reduced thickness h_m in the range from 0.05 to 5. One can see that the results obtained confirm and make more exact the data from Fig. 3 concerning the oscillatory behavior of the diameter as a function of the film parameters. The information about the positions of maxima (the crests of the surface) on the $h-n$ plane is of the most interest. To this end, three curves, which demonstrate that the interpolation of "resonance" conditions was quite satisfactory, are drawn in Fig. 4. These curves are described by the common dependence

$$h(n^2 - \varepsilon_0 \sin^2(0.45\pi/2))^{1/2} = m/2, \qquad (22)$$

where the integer parameter m is the serial number of the "resonance". The behavior of this dependence means that the RAP diameter grows drastically if the phase retardation across the film corresponds to an integral multiple of the half wavelength of light incident upon the film at an angle of $0.45\pi/2$. In addition, Fig. 4 demonstrates how the region diameter diminishes along the crests, if the values of the refractive indices of the film and the substrate come closer.

Thus, the calculations carried out for the shape and the diameter of the RAP confirm both our initial assumptions and experimental results concerning a drastic dependence of the accuracy of the ellipsometric characterization of films on their physical parameters, provided a constant measuring error of ellipsometric measurements themselves. The characterization accuracy becomes worse by more than an order of magnitude, if the "resonance" condition (22) with $m = 1$ is obeyed. As the parameter m grows, the oscillatory character of the dependence is smoothed out, and the characterization accuracy becomes invariably high.

7. Conclusions

The error function of a new type, which has a clear physical meaning and is closely connected to a physical quantity directly measured in experiment, has been introduced. In our opinion, it estimates a mismatch between experimental and simulation results methodically more correctly in comparison with the error functions known earlier.

Making use of the new error function, a procedure, which numerically solves the inverse problem of multiple-angle-of-incidence ellipsometry and evaluates the errors of the solution obtained, has been developed.

On the basis of MAIE experimental data, the boundaries of the region of admissible parameters have been determined for several sections of a porous TiO_2 film.

The numerical calculations have revealed the oscillatory dependence of the accuracy of ellipsometric characterization of the film on the physical parameters of the latter.

The results obtained evidence for the necessity of the inclusion of the numerical procedure that calculates the RAP boundaries into the procedure of solving the inverse problems of MAIE. This scenario seems more practical than an attempt to find the analytical solution of the problem. Moreover, if the measurements result in a film thickness that satisfies condition (22) for the growth of the RAP diameter with a small serial number, then either the laser wavelength should be changed or the method of spectral ellipsometry should be applied.

1. *Azzam R.M.A, Bashara N.M.* Ellipsometry and Polarized Light. — Amsterdam: North-Holland, 1987.
2. *Jenkins T.E.* // J. Phys. D: Appl. Phys. — 1999. — **32**. — P.R45 — R56.
3. *Woollam J.A., Johs B., Herzinger C.M. et al.* // SPIE Proc. CR72. — 1999. — P. 29—58.
4. *Svitasheva S.N.* // Dokl. AN SSSR. — 1991. — **318**, N 5. — P. 1154—1158.

5. *Belyaeva A.I., Galuza A.A., Grebennik T.G., Yuryev V.P.* // Opt. Spektr. — 1999. — **87**, N 6. — P.1041 — 1044.

6. *Petrik S., Smirnova N.P., Frolova O.K. et al.* // Khim. Fiz. Teknhol. Poverkhni. — 2004. — N 10. — P. 90—94.

7. *Born M., Wolf E.* Principles of Optics. — Oxford: Pergamon Press, 1980.

8. *Jackson J.D.* Classical Electrodynamics. — New York: Wiley, 1962.

9. *Landau L.D., Lifshits E.M.* Electrodynamics of Continuous Media. — New York: Pergamon, 1960.

10. *Antonyuk V.N., Dmitruk N.L., Medvedeva M.F.* // Ellipsometry in Science and Technology.— Novosibirsk, 1987. — P. 66—71 (in Russian).

11. *Myhailyk T.A.* Ellipsometry of Superlattices and Disordered Surfaces of GaAs and Si Single-Crystals: Thesis for Ph.D. degree in Physics and Mathematics. — Kyiv, 2000 (in Ukrainian).

Received 11.07.05.
Translated from Ukrainian by O.I. Voitenko

ОЦІНКА ТОЧНОСТІ ВИМІРЮВАННЯ ПАРАМЕТРІВ ТОНКОЇ НЕПОГЛИНАЮЧОЇ ПЛІВКИ ЗА ДОПОМОГОЮ ЕЛІПСОМЕТРІЇ ПРИ БАГАТЬОХ КУТАХ ПАДІННЯ

І.С. Петрик, О.В. Турчин, О.К. Фролова

Р е з ю м е

Визначаючи експериментально параметри тонких непоглинаючих плівок методом еліпсометрії при багатьох кутах падіння було помічено різке падіння точності вимірювання для деяких зразків. З метою дослідження цього ефекту в роботі введено функцію похибок нового типу, що має прозорий фізичний зміст “середнього фотоструму, яким нехтують”, і на її основі побудовано процедуру чисельного розв’язку оберненої задачі еліпсометрії. Обробка експериментальних даних за допомогою цієї процедури дозволила визначити межі області допустимих параметрів для декількох ділянок плівки пористого TiO_2. Крім того, чисельним розрахунком продемонстровано осцилюючу залежність точності еліпсометричних вимірювань характеристик плівки від її фізичних параметрів. Отримані результати вказують на необхідність включення чисельної методики розрахунку межі області допустимих параметрів у процедуру розв’язування оберненої задачі еліпсометрії.